From Surface Equivalence Principle to Modular Domain Decomposition

Florian Muth[1], Hermann Schneider[2], and Timo Euler[3]

1 Introduction

Real-world electromagnetic problems such as mounted antennas often involve multiple electromagnetic scales and properties: These kinds of problems may contain antenna models with extremely detailed structures and complex materials besides electrically very large platforms of hundreds of wavelengths. Potentially, even complete systems, e.g. additionally including the feeding circuits of the antennas, need to be simulated. There are existing meth-

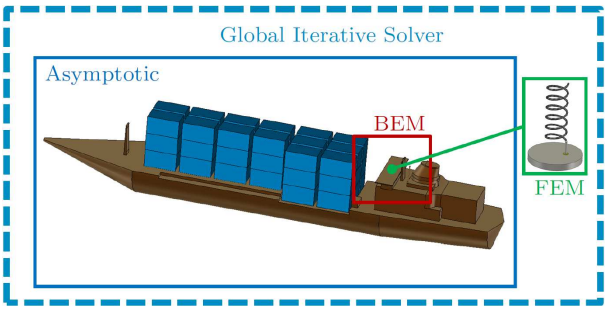

Fig. 1: Complex models, e.g. involving multiple scales, can be decomposed into smaller subdomains to apply the most suitable solver to each subdomain.

ods suitable to solve the full-wave MAXWELL's equations for each part of the described complex problem. E.g. the Finite Integration Technique (Wei-

[1] CST – Computer Simulation Technology AG, Germany Florian.Muth@cst.com ·[2] CST – Computer Simulation Technology AG, Germany Hermann.Schneider@cst.com ·[3] CST – Computer Simulation Technology AG, Germany Timo.Euler@cst.com

land [1977]) or the finite element method (Monk [1992]) could be used for the comparatively small and complex antennas, while a boundary element method (Chew et al. [2001]) or an asymptotic approach (McNamara et al. [1990]) would be more appropriate for the electrically large platform. All these methods have their strengths regarding particular types of electromagnetic problems, but their capabilities are limited, especially if a combination of the mentioned problem types occur.
Here, domain decomposition methods come into play. The goal is to spatially decompose the original model into smaller subdomains and to apply the most suitable method in each subdomain. To obtain the overall solution, a global iterative solver is needed. An example for this approach is depicted in Fig. 1.

The presented project pursues a modular domain decomposition approach to enable the simple integration of existing electromagnetic solvers. Here, the subdomains are coupled via surface currents. This allows for adding arbitrary methods to the developed black box framework, to make use of the full potential of available electromagnetic solvers.

2 Love's Equivalence Principle

The method described in this paper is based on the surface equivalence principle as developed by A. E. H. Love and described in Schelkunoff [1936]. The coupling of the subdomains is realized by exchanging boundary data in terms of surface currents. Love's equivalence principle is illustrated in Fig. 2.

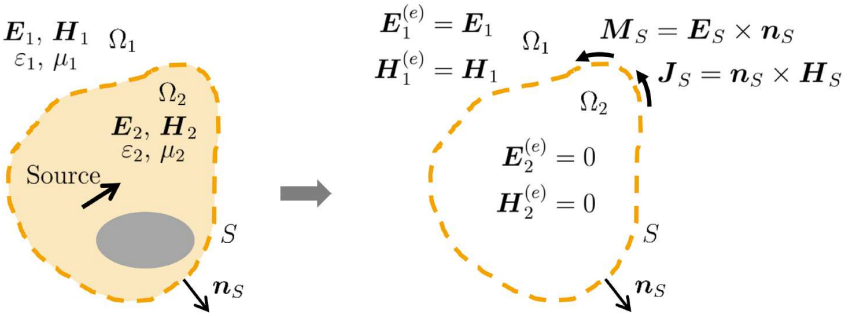

(a) Original model (b) Outer equivalent model

Fig. 2: According to Love's equivalence principle, sources and material distributions enclosed by a surface S in an original model (a) can be replaced by equivalent electric and magnetic surface currents $\mathbf{J}_S$ and $\mathbf{M}_S$ on S to obtain an equivalent model with the same solution outside of S (b).

Let's assume an original model domain Ω is decomposed into two subdomains Ω_1 and Ω_2 by introducing a closed surface S, see Fig. 2(a). $\mathbf{E}_i$ and $\mathbf{H}_i$ are the solutions of the original model for the electric and magnetic fields in subdomain Ω_i. ε_i and μ_i are the permittivity and the permeability of the material in the respective subdomain. The field solution on the surface S is denoted by $\mathbf{E}_S$ and $\mathbf{H}_S$.
According to LOVE's equivalence principle, the sources and material distributions enclosed by surface S can be replaced by equivalent electric and magnetic surface currents $\mathbf{J}_S = \mathbf{n}_S \times \mathbf{H}_S$ and $\mathbf{M}_S = \mathbf{E}_S \times \mathbf{n}_S$. Here, $\mathbf{n}_S$ is the unit normal vector of S pointing outwards. The resulting equivalent model for the outer domain Ω_1 as shown in Fig. 2(b) reproduces the solution of the original model in Ω_1, i.e. $\mathbf{E}_1^{(e)} = \mathbf{E}_1$ and $\mathbf{H}_1^{(e)} = \mathbf{H}_1$, and null fields in Ω_2. In the equivalent model, it is irrelevant what is modelled inside of the surface S, since the fields of the solution are forced to zero anyway.
The same applies for the corresponding inner equivalent model. Equivalent surface currents are defined in the same way on S, but the unit normal vector $\mathbf{n}_S$ is inverted pointing inwards. As for the outer equivalent model this results in null fields in Ω_1 and reproduces the solution of the original model in Ω_2.
Fig. 3 illustrates again the above described principle with the help of a

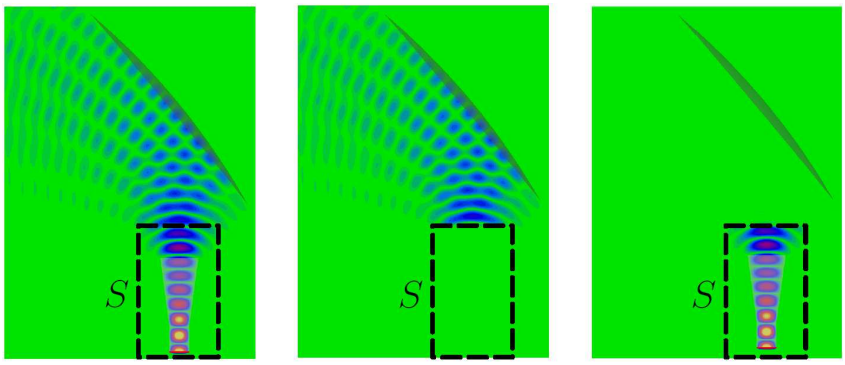

(a) Original model (b) Outer equivalent model (c) Inner equivalent model

Fig. 3: LOVE's equivalence principle is demonstrated by means of a reflector antenna setup using CST MICROWAVE STUDIO®: By monitoring the tangential fields on S in the original model (a), either the inside (b) or the outside (c) of the closed surface S can be replaced by equivalent surface currents.

reflector antenna setup simulated with CST MICROWAVE STUDIO®. Additionally, the inner equivalent model (Fig. 3(c)) is shown besides the original and the outer equivalent models.

3 Iteration Scheme for Modular Domain Decomposition

The principle described in the previous section will be utilized for the black box domain decomposition approach. In this way, the subdomains need only provide surface currents to realize the coupling to the other subdomains. In the end, this will result in an iterative domain decomposition method, which will be explained in the following section.

The reflector antenna model from section 2 is again considered. After decomposing it into the two subdomains Ω_1 and Ω_2, we obtain a typical coupled system. Now, the idea is to solve this coupled system by making use of Love's surface equivalence principle. But, instead of knowing the solution of the original model $\mathbf{E}_S$ and $\mathbf{H}_S$ beforehand, only approximations $\tilde{\mathbf{E}}_S$ and $\tilde{\mathbf{H}}_S$ are available, since the subdomains have to be solved separately. Here, the subdomains can basically be truncated by arbitrary boundary conditions, even transparent boundary conditions can be considered. Additionally, the exchange surfaces can be chosen in different locations. This gives the resulting domain decomposition method a high flexibility in defining the coupling interfaces between the subdomains and allows for the introduction of overlaps between them.
The above approach finally results in the following linear system, whose terms will be explained subsequently:

$$\begin{bmatrix} \boldsymbol{I} & \overline{\boldsymbol{R}}_1 \boldsymbol{A}_1^{-1} \boldsymbol{C}_{12} \overline{\boldsymbol{R}}_2^T \\ \overline{\boldsymbol{R}}_2 \boldsymbol{A}_2^{-1} \boldsymbol{C}_{21} \overline{\boldsymbol{R}}_1^T & \boldsymbol{I} \end{bmatrix} \begin{bmatrix} \overline{x}_1 \\ \overline{x}_2 \end{bmatrix} = \begin{bmatrix} \overline{\boldsymbol{R}}_1 \boldsymbol{A}_1^{-1} b_1 \\ \overline{\boldsymbol{R}}_2 \boldsymbol{A}_2^{-1} b_2 \end{bmatrix} \tag{1}$$

$$\overline{x}_1 = \begin{bmatrix} \tilde{\mathbf{H}}_{S^+}^{(1)} \\ \tilde{\mathbf{E}}_{S^+}^{(1)} \end{bmatrix}; \quad \overline{x}_2 = \begin{bmatrix} \tilde{\mathbf{H}}_S^{(2)} \\ \tilde{\mathbf{E}}_S^{(2)} \end{bmatrix} \tag{2}$$

The unknowns of the system $\overline{x}_1$ and $\overline{x}_2$ are defined on the coupling surfaces between the subdomains. By solving this system iteratively using a GMRES solver (Saad and Schultz [1986]), the solution of the original model on the surface S is obtained. From this, the field solutions in the subdomains can be derived.
Although eq. 1 describes a domain decomposition formally very much alike to e.g. the formulation found in Peng and Lee [2010], it goes far beyond non-overlapping domain decompositions with standard transmission conditions: It features a high flexibility in defining the coupling interfaces and extensions of the subdomains, as described above. In section 4, this flexibility is employed to enhance iteration convergence by introducing overlaps without resorting to e.g. higher order transmission conditions as done in Peng and Lee [2010].
The iteration scheme of the presented method is illustrated in Fig. 4. Boundary data in terms of surface fields is iteratively exchanged between

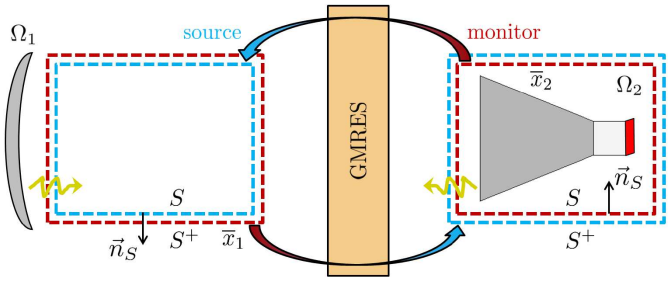

Fig. 4: Boundary data is iteratively exchanged by monitoring surface fields, which are then imprinted as current sources in the other domain. By solving the corresponding linear system using e.g. a GMRES solver, the solution of the original model is obtained.

the subdomains, where each iteration mainly consists of three parts. First, the monitored surface fields $\overline{x}_j$ from subdomain Ω_j are transformed into a current source for subdomain Ω_i, represented by the operator $\boldsymbol{C}_{ji}\overline{\boldsymbol{R}}_i^T$. Afterwards, subdomain Ω_i is solved by applying its inverted system operator $\boldsymbol{A}_i^{-1}$. In the last step, the operator $\overline{\boldsymbol{R}}_i$ restricts the obtained solution to the corresponding coupling surface S. In practice, the last step is realized by monitoring the fields on the coupling surface. After each iteration, the feedback is exchanged between the subdomains to take into account the influence of the other parts of the model.
As shown in Fig. 4, the surfaces where the fields are monitored and the currents are imprinted do not coincide. This follows from the jumping fields due to the imprinted electric and magnetic currents.

4 Investigations

The area of application of the presented black box framework mainly comprises models with a small number of user-defined, coupled subdomains as is the case for antenna placement scenarios. Here, the priority is not on scalability regarding the number of subdomains, but on the flexibility of the overall domain decomposition framework.
For first investigations, an “array” of two patch antennas is considered. The setup of this model and how it is decomposed into two subdomains is illustrated in Fig. 5. Each of the patch elements is simulated with CST’s finite element frequency domain solver using an absorbing boundary condition (ABC). By shifting the coupling interfaces, non-overlapping ($d = 0$) as well as overlapping ($d > 0$) setups can be realized. In the latter case, each subdomain is extended towards the other one by modelling the structure of the

original model in the overlap region. The discretizations of the subdomains can be chosen independently of each other and don't need to match in the overlap region nor at the coupling interfaces.

For the validation of the results of the presented domain decomposition method, the absolute value of the electric field is evaluated along the array axis and slightly above the surface of the patch elements for $d = 0$. In Fig. 6, the corresponding curves are depicted showing the smooth transition from one subdomain to the other at $x = -3\,\mathrm{cm}$. Furthermore, the results precisely match the solution of the original model.

An interesting aspect for future investigations is the relationship between the relative residual of the global iterative solver and the error of the quantities of interest. For the investigated model ($d = 0$), the absolute error of the S-parameter as the quantity of interest is already smaller than 10^{-3} after the first iteration, which is sufficient for typical engineering applications (Fig. 7).

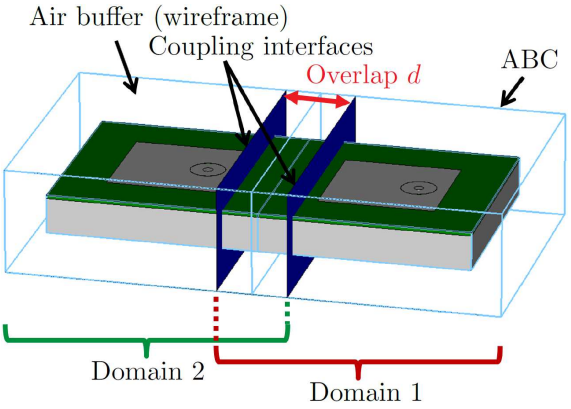

Fig. 5: The 1x2 patch antenna array is decomposed into two subdomains, each calculated by CST's finite element frequency domain solver. The subdomains are truncated by an absorbing boundary condition (ABC) and can partly overlap by a size d.

As pointed out in section 3, overlaps can be used to accelerate the convergence of the global iterative solver. Fig. 8 compares the convergence of the relative residual of the global iterative solver for different overlap sizes d. The larger the overlap size the faster the presented method converges. At the same time, there is no significant performance drawback, since the overlaps are still quite small in terms of the wavelength λ. E.g. $d = 4 \times 10^{-2}\,\lambda$ corresponds to an overlap size of approximately one mesh cell layer and reduces the number of iterations from 7 to 4 to reach a relative residual smaller than 10^{-3}.

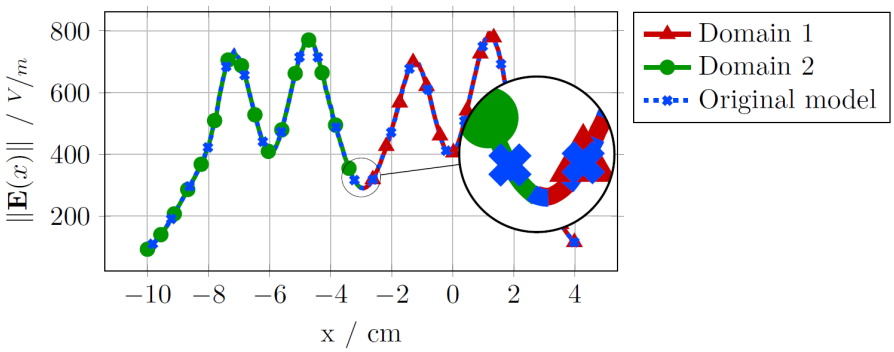

Fig. 6: The results of the presented method precisely match the solution of the original model for the non-overlapping setup ($d = 0$). Especially, a smooth transition between the subdomains at $x = -3\,\text{cm}$ can be observed.

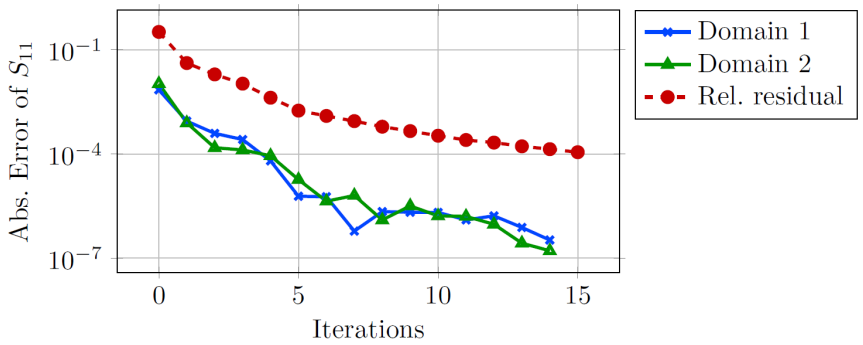

Fig. 7: Comparison of the relative residual of the global iterative solver with the absolute error of the S-parameter for the non-overlapping setup ($d = 0$): For typical engineering applications, an absolute error smaller than 10^{-3} is already sufficient. The value from the fifteenth iteration was taken as reference.

5 Discussion and Conclusion

This paper has presented a domain decomposition approach, which is suitable for electrically large and complex setups. The main advantage is its modularity due to the coupling of the subdomains via surface currents motivated by the equivalence principle. The resulting black box framework allows for any numerical method in each subdomain. Another feature is the high flexibility in defining the coupling interfaces between the subdomains. In this way, overlapping setups can easily be introduced.
Promising results regarding the coupling of finite element subdomains were shown. The presented method was proven to converge for both the non-

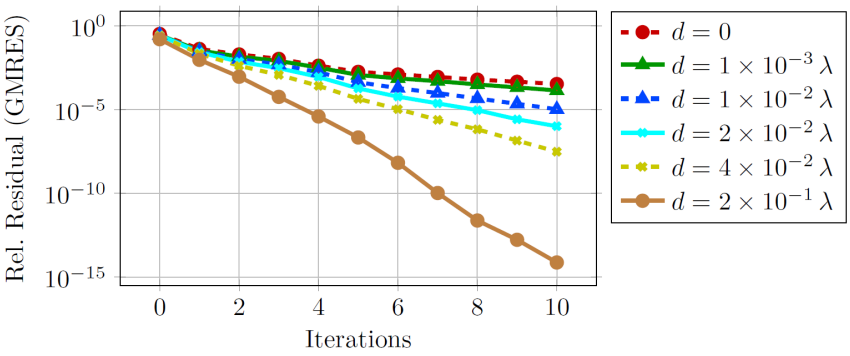

Fig. 8: The convergence of the presented method can be accelerated by introducing an overlap $d > 0$. There is no significant performance drawback, since the overlap size is in the range of a fraction of the wavelength λ.

overlapping and the overlapping setup. By introducing a small overlap of a fraction of a wavelength, the convergence of the method could be accelerated drastically.

References

Weng Cho Chew, Jian-Ming Jin, Eric Michielssen, and Jiming Song. *Fast and Efficient Algorithms in Computational Electromagnetics*. Artech House Publishers, 2001.

D.A. McNamara, C.W.I. Pistorius, and J.A.G. Malherbe. *Introduction to the Uniform Geometrical Theory of Diffraction*. Antennas and Propagation Library. Artech House, 1990.

Peter Monk. A finite element method for approximating the time-harmonic Maxwell equations. *Numerische Mathematik*, 63(1):243–261, dec 1992.

Zhen Peng and Jin-Fa Lee. Non-conformal domain decomposition method with second-order transmission conditions for time-harmonic electromagnetics. *Journal of Computational Physics*, 229(16):5615–5629, aug 2010.

Youcef Saad and Martin H. Schultz. GMRES: A Generalized Minimal Residual Algorithm for Solving Nonsymmetric Linear Systems. *SIAM Journal on Scientific and Statistical Computing*, 7(3):856–869, 1986.

S. A. Schelkunoff. Some equivalence theorems of electromagnetics and their application to radiation problems. *Bell System Technical Journal*, 15(1): 92–112, 1936.

Thomas Weiland. A discretization model for the solution of Maxwell's equations for six-component fields. *Archiv fuer Elektronik und Uebertragungstechnik*, 31:116–120, 1977.